Inorganica Chimica Acta, *187* (1991) 107–114

An EPR and electronic spectroscopy study of intermediates in a mono *o*-nitro substituted iron porphyrin reaction with iodosylbenzene

Marilda das Dores Assis, Osvaldo Antonio Serra, Yassuko Iamamoto*
Departamento de Quimica, FFCLRP-USP, Av. Bandeirantes 3900, CEP 14049, Ribeirão Preto, SP (Brazil)
and Otaciro Rangel Nascimento
Departamento de Fisica, IFQSC-USP, C.P. 369, CEP 13560, São Carlos, SP (Brazil)

(Received January 3, 1991)

Abstract

We have studied the intermediates generated by the oxidation of the bromo[5-*o*-nitrophenyl,10,15,20-triphenylporphyrin)iron(III)] complex with iodosylbenzene in dichloromethane. We previously observed that the oxidation of cyclohexane with this system gave a 60% yield of cyclohexanol based on iodosylbenzene. The intermediate species were studied by visible spectra at −60 °C and at room temperature, and also by electron paramagnetic resonance (EPR). The electronic spectra, after reaction occurred between 0–15 s, indicate the formation of a Fe(IV) species and dimeric species; at 10–15 s a green solution was also obtained. The EPR spectra in the same conditions exhibit a signal at $g = 2.0016$, assigned to a radical. These results gave rise to the conclusion that the catalytic species in this system is the dimeric ferryl porphyrin π-cation radical, $(P)Fe^{IV}–O–Fe^{IV}(O)(P^{\cdot+})$ (P is the porphyrin). Through the dimer formation the orthogonality of the ferryl-iron is retained (D_{4h} symmetry) preventing magnetic coupling with the porphyrinic ring radical. Thus, this radical is observed by EPR. These results do not exclude the possibility of the existence of a monomeric ferryl porphyrin π-cation radical as the catalytic species.

Introduction

There have recently been considerable efforts to isolate and characterize the high valence oxoiron-porphyrin complex as an intermediate in synthetic catalytic processes of oxygenation such as hydrocarbon hydroxylation [1–7]. The interest in these systems is due to their capacity to *mimetize* enzymes such as cytochrome P-450, responsible for important reactions, such as the activation of the alkane C–H bond in living organisms [8–10].

Reaction of cytochrome P-450 enzymes with various oxygen transfer agents such as peracids and iodosylarenes leads to an enzyme oxidant having characteristics similar to the oxidant produced via the biochemical pathway. A remarkable similarity exists between the products obtained with the oxidation reactions carried out with synthetic iron(III)-porphyrins with cytochrome P-450 and these oxygen atom transfer agents [11, 12].

The main reasons for using metalloporphyrins as catalysts are to understand the essential steps in the catalytic cycle of P-450 better and the necessity of introducing new effective synthetic catalysts which are selective to hydroxylate saturated hydrocarbons important in industrial processes.

An oxidant species has been proposed as an active intermediate in the catalytic cycle of cytochrome P-450 analogous to horseradish peroxidase and catalase enzymes whose structures have been identified as high-valent oxoironporphyrin complexes, ferryl porphyrin π-cation radicals, $(^{\cdot+}P)Fe^{IV}(O)$ [13–16].

We have studied the intermediates generated by the oxidation of the bromo[(5-*o*-nitrophenyl,10,15,20-triphenylporphyrinato)iron(III)] complex with iodosylbenzene. This iron porphyrin was synthesized and characterized as a μ-oxo dimer, its more stable species. The interest in this complex is due to the fact, recently observed by us [17], that it is able to oxidize cyclohexane to cyclohexanol selectively with a yield of 60%. If we use the chloro[(5,10,15,20-tetraphenylporphyrinato)iron(III)] complex, other conditions remaining the same, this yield is only 30%. The nitro group appears to stabilize the catalytic species of the reaction, increasing the reactivity with the hydrocarbon and promoting the dimerization.

*Author to whom correspondence should be addressed.

0020-1693/91/$3.50

© 1991 — Elsevier Sequoia, Lausanne

The high-valent iron complexes are very reactive and have been obtained only at low temperatures. Observation of transients in visible (Vis) and electron paramagnetic resonance (EPR) spectra, during the oxidation reactions, has provided insights into the chemistry of the one- and two-electron oxidized species of this iron porphyrin, as well as other porphyrinato iron complexes currently used to probe mechanisms of biological oxidations.

Experimental

Physical measurements

Visible spectra were obtained on a Perkin-Elmer Coleman 575 spectrophotometer. The low temperature spectra were obtained in a 0.6 mm pathlength cuvette in a dewar from Kontes. The dewar temperature was maintained between −60 to −77 °C by methanol equilibrated previously in a dry ice/methanol bath. For detection of the Soret band the solutions were diluted approximately 6 times. EPR spectra were recorded with a Varian E-109 spectrometer operating in the X-band frequency using the variable temperature accessory model E-257 from Varian.

Intermediates

Two types of experiments were performed as follows:

Procedure 1. The intermediates generated in reactions with the porphyrin dissolved in CH_2Cl_2 ($\sim 5\times10^{-3}$ M) were added to iodosylbenzene in CH_2Cl_2 ($\sim 2\times10^{-2}$ M). After the programmed time, the reaction was inhibited by freezing at −77 °C. This solution was diluted with CH_2Cl_2 previously cooled and transferred to the cuvette with a cold 'Pasteur' pipet.

Procedure 2. To control the reaction starting from zero time, the solutions of iron porphyrin and iodosylbenzene were mixed at −77 °C. The reaction was followed by taking the reaction vessel out of the dewar and submitting it to an ultrasound laboratory cleaner (Minison-Thornton), then replacing it in the dewar. The green intermediate was generated after 15 s at room temperature and cooled again to −77 °C.

Syntheses

The 5-*ortho*-nitrophenyl,10,15,20-triphenylporphyrin was prepared according to the method of Collman *et al.* [18] but in propionic acid following Adler *et al.* [19], purified by silica column chromatography and eluted with benzene/cyclohexane (1:1), as the second band.

The iron insertion in the porphyrin was done with $FeBr_2$ in dimethylformamide [20]. The iron porphyrin was purified by alumina column chromatography with CH_2Cl_2 as solvent.

The solvents were purified by normal procedures; the iodosylbenzene obtained by hydrolysis of iodosylbenzenediacetate [21]. The grade of iodosylbenzene was determined by iodometry to be 98%.

Results

Syntheses and characterization

The use of acetic acid instead of propionic acid in the synthesis of iron porphyrin gave no better yield, but gave a more crystalline material, easily purified. The yield of the synthesis considering the pyrrol was 3%. The visible spectra data for the compounds are given in Table 1. The iron insertion resulted in a μ-oxo dimer, $[Fe(o\text{-}NO_2\text{-}\phi\phi_3P)]_2O$, characterized also by the infrared transitions at 870 cm^{-1} (Fe–O–Fe), and by the absence of a signal in the EPR spectra. The monomer, $[Fe(o\text{-}NO_2\text{-}\phi\phi_3P)]X$, was obtained by treating the dimer with bromidric or chloridric acid. The monomer EPR spectrum is due to high spin Fe(III) ($S=5/2$), Fig. 1(a). The dimer is the more stable compound in the synthesis and purification procedures employed.

Intermediate studies

The 'zero time' was considered as the instant of mixing of the two previously cooled reagents. In the EPR spectra (~ -170 °C) the system is frozen. In the visible spectra (−60 °C) we have a solution and the reaction could continue, although slowly. In the absence of substrate the catalytic species could attack the solvent giving CO_2 and HCl.

Electron paramagnetic resonance

Figure 1 presents the EPR spectra of three experiments with the monomer at 'zero time'. Figure 1(a) shows a signal at $g=5.98$ (Fe(III), $S=5/2$), showing that no reaction occurred; 1(b) shows weak signals at $g=5.98$ and 2.0, indicative of a initial step with new EPR silent species; 1(c) presents a intense signal at $g=2.0016$ ($\Delta H=42$ G) and very weak ones at $g=4.29$ and 5.98. In Figure 2 it is important to observe also the signal evolution at the beginning of the reaction (a, b and d); Fe(III), $g=5.98$ practically disappears and $g=2.0016$ starts to appear. Later, $g=5.98$ is still diminishing and 2.0016 stabilizes. This behavior is an indication of the formation of an EPR silent species that leads to the species responsible for the signal at 2.0016. In all experiments the reaction was carefully followed by observing the signals in

TABLE 1. Electronic absorption spectra of porphyrins and iron porphyrins

Compound	Wavelength maxima (nm) ($\times 10^{-3}$ M^{-1} cm^{-1})						Reference
TPP[a]	419(470)	515(18.7)	548(8.1)	592(5.3)	647(3.4)		22
o-NO_2-$\phi\phi_3P$[b]	416[d]	513[d]	547[d]	588[d]	645[d]		19, this work
|Fe(TPP)|Cl[c]	378(58)	415(108)	509.5(13)	577.5(33)	656.5(2.8)	690.5(3.1)	23
|Fe(o-NO_2-$\phi\phi_3$P)|Cl[b]	376[d]	415(135)	510(12.5)	578(33)	657[d]		this work
|Fe(o-NO_2-$\phi\phi_3$P)|$_2$O[b, e]	408(150)		571(17.5)	612(7.38)			this work

[a]C_6H_6. [b]CH_2Cl_2. [c]$CHCl_3$. [d]The extinction coefficients were not determined. [e]The extinction coefficients are based on the molecular weight of the dimer.

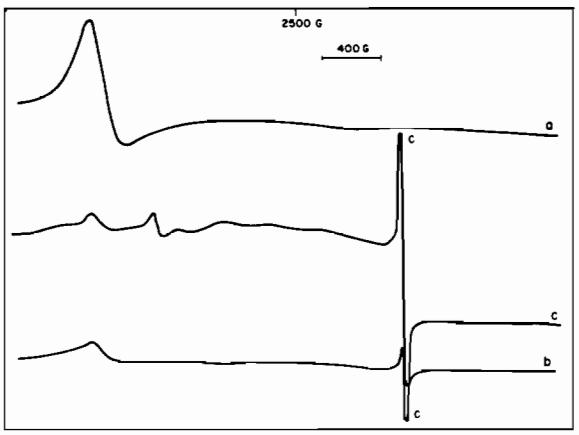

Fig. 1. EPR spectra of the reaction mixture of [Fe(o-NO_2-$\phi\phi_3$P)]X and ϕIO in CH_2Cl_2 immediately after the addition ($t \sim 0$ s). (a) [Fe(o-NO_2-$\phi\phi_3$P)]Cl (1.3×10^{-3} M) with ϕIO (6.2×10^{-3} M); recorded at -150 °C, gain 5.0×10^3; (b) [Fe(o-NO_2-$\phi\phi_3$P)]Cl (1.6×10^{-3} M) with ϕIO (8.2×10^{-3} M); recorded at -180 °C, gain 4.0×10^3; (c) [Fe(o-NO_2-$\phi\phi_3$P)]Br (1.1×10^{-3} M) with ϕIO (7.7×10^{-3} M), recorded at -180 °C, gain 4.0×10^3. All traces were recorded with 10 mW microwave power at 9.12 GHz and 10 G modulation.

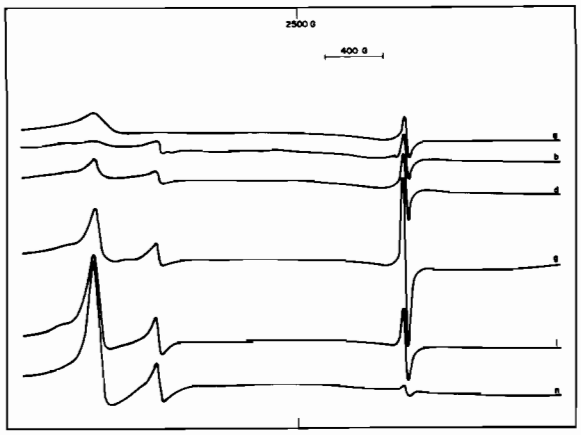

Fig. 2. EPR spectra of the reaction between CH_2Cl_2 solutions of [Fe(o-NO_2-$\phi\phi_3$P)]X (1.6×10^{-3} M) and ϕIO (8.2×10^{-3} M), using agitation with ultrasound. All traces were recorded at -180 °C; with 10 mW microwave power; gain 4.0×10^3; at 9.128 GHz; 10 G modulation, after the reaction times, with 2 s intervals: (a) ~0 s; (b) 2 s; (d) 6 s; (g) 12 s; (l) 35 s; (n) 65 s. Traces c, e, f, h, i, j, k, m, have been omitted.

short time intervals (2, 5, 10 or 30 s). Figure 2 shows an example of the reaction evolution and we may make two observations: partial (50%) recovering of Fe(III) as indicated by increasing of the signals $g=5.98$ ($S=5/2$) and $g=4.29$ ($S=5/2$ with rhombic distortion) and an increasing intensity of the signal at $g=2.0016$ reaching a maximum at 10 s and disappearing after 2 min, indicative of an intermediate species. This behavior was the same when the dimer was the starting material; however, the initial EPR spectra had no signals due to the antiferromagnetic coupling via the μ-oxo bridge [24]. The reaction with the dimer is slower, indicated by the maximum at $g=2.0016$ after 3 min and its collapse after 10 min (Fig. 3). In the presence of the substrate (C_6H_{12}), for both monomer and dimer as catalyst, the species with $g=2.0016$ vanishes in half the time required by the compound with no substrate, being indicative of the participation of this species in the hydroxylation catalytic process.

The anisotropic signal at $g=4.29$ is at the limit for rhombic symmetry of the system $S=5/2$ [25]. This signal is assigned to the iron porphyrin species with a bonding between the Fe(III) and the pyrrolic nitrogen via an oxygen bridge [7, 26]. The signal at $g=2.0016$ is better characterized in the inset of Fig. 4 and is located in the expected g interval (1.999–2.006) for porphyrin radicals [27]. The signal is very intense in the EPR of the green species formed after 15 s of reaction at room temperature of the monomeric porphyrin and iodosylbenzene (Fig. 4). Saturation of the signal did not occur even at a microwave power of 200 mW, as would be expected for a free radial. This radical was not observed in control experiments in the absence of porphyrin. The signal intensity and the yield of the hydroxylated

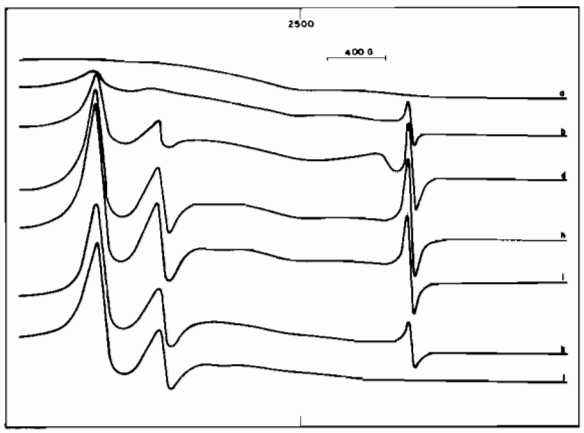

Fig. 3. EPR spectra of the reaction between CH_2Cl_2 solutions of [Fe(o-NO_2-$\phi\phi_3$P)]$_2$O (5.5×10^{-4} M) and ϕIO (6.4×10^{-3} M) using agitation with ultrasound. All traces were recorded at −150 °C; 10 mW microwave power; gain 1.25×10^4; at 9.132 GHz and 10 G modulation; after the reaction times, with 30 s intervals: (a) ~0 s; (b) 30 s; (d) 90 s; (h) 215 s; (i) 275 s; (k) 395 s; (l) 605 s. Traces c, e, f, g, j, have been omitted.

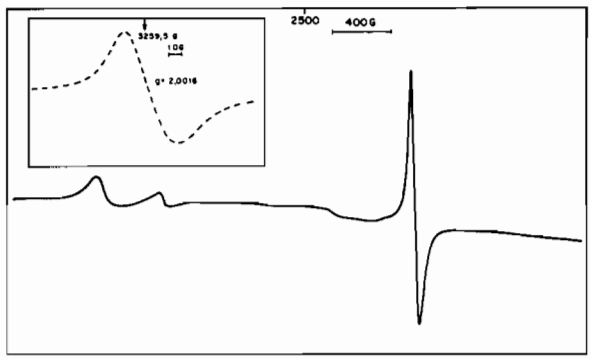

Fig. 4. EPR spectrum after 15 s of the reaction of [Fe(o-NO_2-$\phi\phi_3$P)]Cl (2.1×10^{-3} M) with ϕIO (9.4×10^{-3} M) in CH_2Cl_2 (green solution); recorded at −155 °C; 10 mW microwave power; gain 3.2×10^3, at 9.132 GHz and 10 G modulation. Inset: EPR signal generated in the reaction between CH_2Cl_2 solutions of [Fe(o-NO_2-$\phi\phi_3$P)]Br (1.5×10^{-3} M) and ϕIO (2.8×10^{-3} M) at −164 °C, 10 mW microwave power; gain 5.0×10^3 M; 5.0 G modulation; at 9.132 GHz.

product (cyclohexanol) was increased by 25% when ultrasound was used during the reaction. It is known that ultrasound is able to promote and accelerate organic reactions in which free radical intermediates are produced chemically subsequent to the ultrasound effect [28, 29]. These observations, and the fact that we do not observe hyperfine splitting due to the nuclear magnetic interaction with neighbor atoms such as iodine ($S=5/2$) (from iodosylbenzene) and chlorine ($S=3/2$) (from the solvent), led us to believe in a π-cation radical produced by the oxidation of the porphyrinic ring. The bandwidth too wide (42 G) for a radical and the non-saturation of the signal are due to an interaction with the iron-spin. The green color of the solution (15 s reaction) is also attributed to a ferryl porphyrin π-cation radical [1]. A ferryl porphyrin π-cation radical has been postulated as a catalytic intermediate in oxidation reactions in synthetic systems [1] as well as such biological ones as horseradish peroxidase (compound I) [15] and catalase activities [16]. In synthetic systems, there is no evidence in the literature of an observation of the porphyrinic radical signal, due to coupling of the spin radical with Fe(IV) [1, 30]. In the biological system a weak signal due to the radical is observed, however, only at very low temperatures from 4 to 10 K [31]. Thus, this is the first time that the detection of a signal is observed and related.

Visible absorption at room temperature

The spectra recorded at room temperature, following the oxidation, gave important information free from interference caused by the freezing of the system. However, the response rate of the chart recorder limited the observation of the species that react more quickly.

Figure 5 shows two spectra recorded during the reaction, which are characteristic of the ferryl porphyrin π-cation radical. In both spectra the Soret band is less intense and shifted to lower wavelength (~405 nm). In the 500 to 700 nm region the bands are poorly defined or the intensity absorption is increased in this region [2, 32, 33]. A band at 650 nm is the spectroscopic evidence of the porphyrinic radical [1, 2, 34]. In our system this band is always associated with bands at 571 and 612 nm (assigned to the dimer) as shown in Fig. 6.

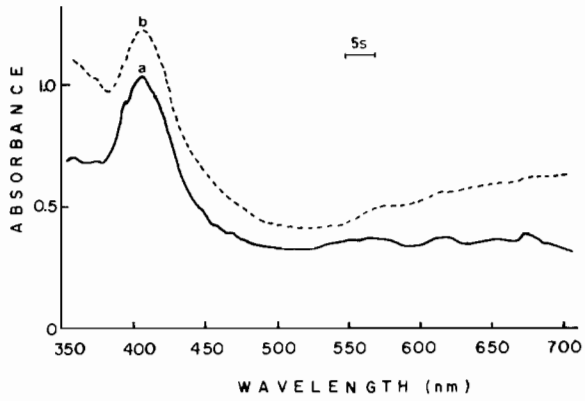

Fig. 5. (a) Visible spectrum at room temperature of the reaction of CH_2Cl_2 solutions of [Fe(o-NO_2-$\phi\phi_3$P)]X (2.3×10^{-3} M) and ϕIO (1.2×10^{-2} M) (green solution); recording started at 14 s (——). (b) Visible spectrum at room temperature of the reaction of CH_2Cl_2 solutions of [Fe(o-NO_2-$\phi\phi_3$P)]X (2.3×10^{-3} M) and ϕIO (1.2×10^{-2} M); recording started at 90 s (– – –).

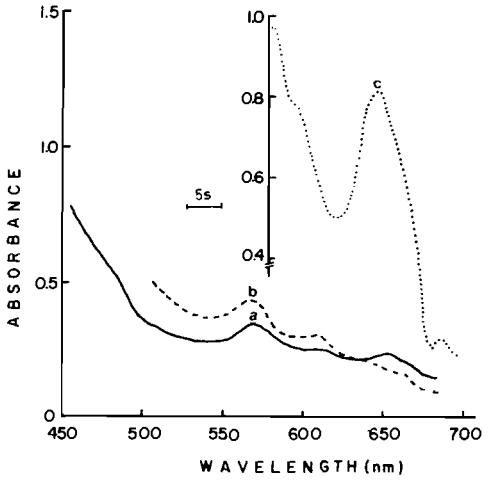

Fig. 6. Visible spectra recorded at room temperature for the reaction of the [Fe(o-NO_2-$\phi\phi_3$P)]X (1.8×10^{-3} M) and ϕIO (8.8×10^{-3} M): (a) recording started at 19 s in 450 nm (——); (b) recording started at 88 s in 500 nm (– – –). (c) Recording started at 14 s in 550 nm (· · · · ·) for the reaction of [Fe(o-NO_2-$\phi\phi_3$P)]X (2.3×10^{-3} M) and ϕIO (1.2×10^{-2} M) CH_2Cl_2 solutions (green solution).

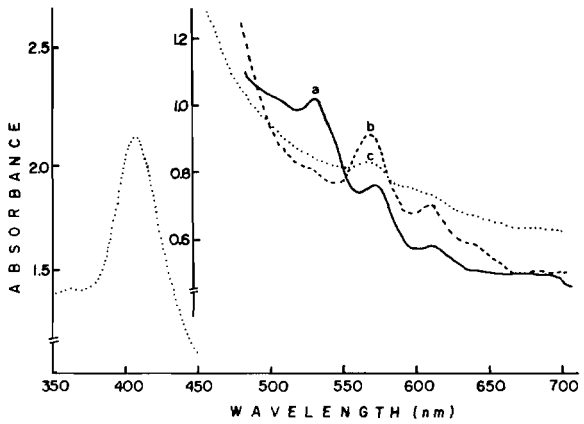

Fig. 8. Visible spectra recorded at −60 °C for the reaction of (a) [Fe(o-NO_2-$\phi\phi_3$P)]Cl (1.5×10^{-3} M) and ϕIO (8.6×10^{-3} M) in CH_2Cl_2 immediately after the mixture of the reagents (orange solution) (——); (b) [Fe(o-NO_2-$\phi\phi_3$P)]Br (1.6×10^{-3} M) and ϕIO (8.2×10^{-3} M) in CH_2Cl_2 after 22 s (– – –) of the reaction (green solution) and (c) diluted ~10 times (· · · · ·).

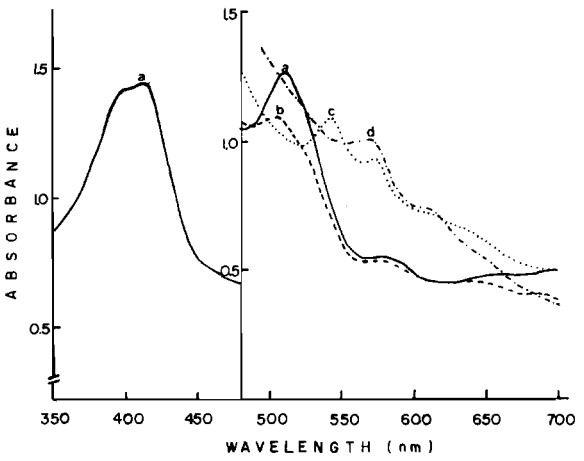

Fig. 7. Visible spectral changes recorded at −60 °C for the reaction of [Fe(o-NO_2-$\phi\phi_3$P)]Cl (2.8×10^{-3} M) and ϕIO (1.2×10^{-2} M) in CH_2Cl_2 and ultrasound, after the reaction times: (a) 0 s (——); (b) 15 s (– – –); (c) 50 s (· · · · ·); (d) 180 s (– · –). For Soret band in (a) the solution was diluted ~10 times.

Visible absorption at low temperature

Lowering the temperature to −60 °C stabilized the intermediate species, making possible a more systematic study of these species. However, the 'freeze–thaw' during data acquisition modifies the reaction rates. Figure 7 presents a reaction evolution with the monomer. At 'zero time' the Soret is already splitted with the maxima at 400 and 417 nm; the 510 nm band is broadened with a new shoulder at 530 nm; and with the disappearance of the 510 nm band a new more intense band is manifest at 542 nm.

Sometimes, 1 or 2 s after the mixing of the reagents at −77 °C, an intense orange color is observed. The spectrum of this solution (Fig. 8(a)) shows a 530 nm band associated with dimeric bands (571 and 612 nm). After 15 s the color changes to green. Figure 8(b) and (c) shows characteristic spectra of the green species. The bands at 408, 571 and 612 nm are characteristic of dimeric species and are associated to weak bands at 530 and 630–650 nm.

When the dimer was the starting material, it was possible to observe at 'zero time' absorptions at 571 and 612 nm, with shoulders at 530, 650 and a weak band at 690 nm. As the reaction proceeds, the shoulder at 530 nm disappears and a new band of medium intensity appears at 542 nm, with a Soret at 421 nm (Fig. 9). These bands could be associated with a Fe(IV) species [2, 6, 35].

Discussion

We propose the following route for the oxidation reaction of the monomeric iron porphyrin, (P), by iodosylbenzene, (ϕIO).

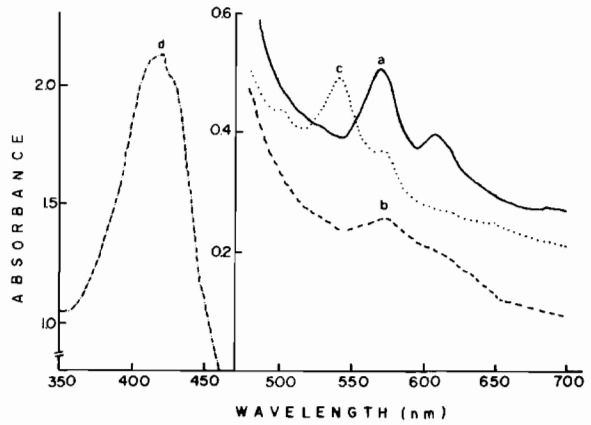

Fig. 9. Visible spectral changes recorded at −60 °C for the reaction in CH_2Cl_2 of $[Fe(o\text{-}NO_2\text{-}\phi\phi_3P)]_2O$ (9.9×10^{-4} M) and ϕIO (1.0×10^{-2} M) with ultrasound, after the reaction times: (a) 0 s (——); (b) 7 s (– – –); (c) 17 s (· · · · ·); (d) 37 s (– · –), after dilution (~10 times).

Route I

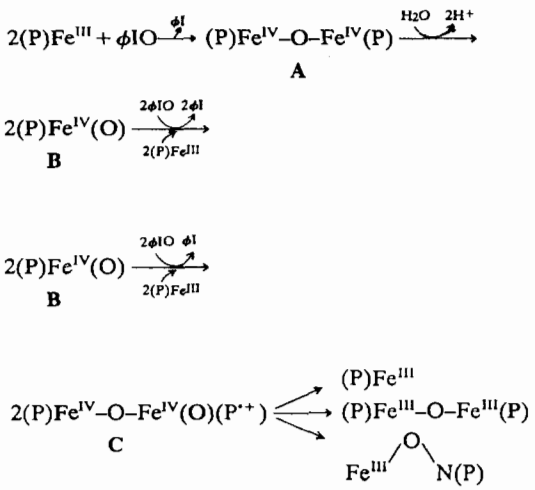

The reaction progress with the monomer (Fig. 2(a) and (b)) shows clearly the step in which the Fe(III) porphyrin is being depleted to yield an EPR silent intermediate. Monomeric and dimeric species with Fe(IV) in our experimental conditions are EPR silent, **A** and **B**, which subsequently transform to a radical species. The radical signal disappears in a few seconds. The species with a rhombic symmetry, Fe^{III}–O–N(P), formed as one of the reaction products, is responsible for the signal at $g=4.29$.

As shown in Figs. 6–8, the characteristic bands in the visible spectra of the dimer (408, 571 and 612 nm) are present at the beginning of the reaction and persist in the Fe(III) or Fe(IV) dimer spectra. The porphyrin is responsible for the most intense bands. However, the presence of a radical localized in the porphyrin will demonstrate considerable spectra modifications. In our system, it was possible to detect visible spectra of the dimer associated to 630 (Fig. 8(b)) and 650 nm (Fig. 6(a)) bands. These bands are ascribed to a porphyrinic radical which agrees with the EPR signal ($g=2.0016$). The Vis and EPR data indicate the presence of this radical in a dimeric species, which is the main catalytic species, **C**. In the presence of the substrate (cyclohexane) the radical life time in EPR spectra is reduced to half. When ultrasound is used, both the radical signal and the yield of cyclohexanol are increased significantly. The catalytic intermediate proposed in the literature [1, 4, 6] for oxidation in similar systems is a ferryl porphyrin π-cation radical. Possibly this radical is coupled antiferromagnetically with Fe(IV), resulting in an effective spin of $S=3/2$, leading to the collapse of the radical signal in the EPR spectra through a very efficient relaxation mechanism. The observation of the signal at $g=2.0016$ indicates a break of this coupling to the radical geometry or to a change in the relaxation mechanism. When the orthogonality of the 3d orbitals of the iron is preserved, there is no overlap with the porphyrin orbitals, such that the spin–spin coupling by exchange is inhibited. In the complex $Fe(OClO_3)_2(TPP^{\cdot})$ the iron orthogonality is preserved and no overlap occurs with the orbitals of the porphyrinic radical despite their close proximity. In the $FeCl(SbCl_6)(TPP^{\cdot})$ the pentacoordinated iron atom is out of plane resulting in non-orthogonality of the orbitals and allowing the coupling [36, 37]. In our case the orthogonality is retained through the formation of a μ-oxo dimer in which the 5th and 6th ligands of the ferryl-iron are the oxygen atoms of the μ-oxo bridge and of the ferryl. These ligands sustain Fe(IV) in the porphyrin plane (D_{4h}), preventing magnetic coupling with the porphyrinic ring. However, the iron proximity allows a magnetic dipole interaction causing a broadening of the radical signal ($\Delta H=42$ G). The dimerization tendency is increased, in this case, by the presence of the nitro group, despite preliminary results with $(FeTPP)_2O$ that indicate the same effect.

Felton *et al* [32] and Phillippi and Goff [33] electrochemically oxidized (one electron) the dimers $(FeTPP)_2O$ and $(FeOEP)_2O$, observing a similar signal at $g=2.0$ with a band width of 30 G. These iron porphyrins, oxidized in the monomeric form, present no signal in the EPR spectra. The non-observation of the $g=2.0$ signal in models of cytochrome P-450, described in the literature, is because these compounds are sterically hindered, not allowing formation of the dimers, which are considered inactive as catalyst [38, 39].

The dimer inertia as catalyst appears only at the beginning of the reaction. The yield of cyclohexanol

is compared using the monomer and the dimer as catalysts, after 3 and 30 min of reaction. After 3 min, the yield with the monomer was 30% and with the dimer only 15%; after 30 min, both gave 50% [17]. This dimer inertia is also observed in its EPR spectra at 'zero time', and in the relatively longer time necessary to reach the maximum value of the $g=2.0$ signal. The evolution of the signals for the dimer was identical with that for the monomer, indicating that both have the same intermediate species. For the dimeric porphyrin, [Fe(*o*-NO_2-$\phi\phi_3$P)]$_2$O, a similar mechanism could be proposed, in which the ϕIO is initially bound to the dimer. This is the determining step, in agreement with the initial inertia of the system using the dimer as catalyst. Another possibility is the change of an oxygen atom from the μ-oxo bridge with the oxygen from ϕIO, resulting in a double-bridged complex (type **1**). Reactions with μ-oxo bridge exchange have been observed using oxygen isotopes [40].

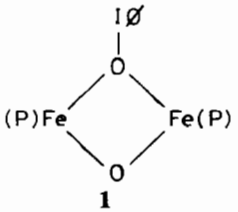

1

The results do not exclude the possible existence of a monomeric ferryl porphyrin π-cation radical (**D**) as the catalytic specie (route II or III). The presence of this radical is identified in Fig. 5 where the Soret band is diminishing and the bands at 500–700 nm are increasing, in agreement with the literature [2, 32, 33].

Route II

$$2(P)Fe^{III} + \phi IO \xrightarrow{\phi I} \underset{\mathbf{A}}{(P)Fe^{IV}\text{–}O\text{–}Fe^{IV}(P)} \xrightarrow{(P)Fe^{III}}$$

$$\underset{\mathbf{D}}{Fe^{IV}(O)(P^{+})} \longrightarrow \text{products}$$

Route III

$$(P)Fe^{III} + \phi IO \xrightarrow{\phi I} \underset{\mathbf{D}}{Fe^{IV}(O)(P^{\cdot+})} \longrightarrow \text{products}$$

Most of the experiments gave evidence for route I. In some experiments it was also possible to detect at 'zero time' a bright orange colored species that quickly changed to green. The spectrum data (Fig. 8(a)) indicate that the orange intermediate is the species **A**, which is the precursor of the green species **C**. It was also possible to detect an intense band at 542 nm (Figs. 7(c) and 9(c)) ascribed to species **B** [35].

Recent data reported in the literature agree that the catalytic species is a dimer porphyrinic radical. A species of type **C** is proposed as an intermediate for the reaction between *p*-cyano-*N*,*N*-dimethylaniline-*N*-oxide and the μ-oxo dimer (FeTPP)$_2$O [41]. The authors also postulate the ferryl porphyrin π-cation (**D**) as the catalytic species formed in a side reaction. Kelly and Yasui [42] relate the presence of a dimer (like **A**) as an intermediate species in heme oxidation with an oxygen donor at ϕIO.

Water participation is important for the formation of the catalytic species (route I). In the presence of water the EPR radical signal was intensified. Also, the yield of cyclohexanol diminished (by 15 to 20%) if ϕIO and solvent are freshly prepared and dried [17].

Possible explanations for the fact that we observe a radical signal in the EPR spectra and a high yield of cyclohexanol with our catalyst, compared to (FeTPP)Cl are the following:

(1) the *ortho* nitro group, being an electron acceptor, stabilizes the porphyrinic radical through the polarization of the electron cloud over the ring decoupling the iron d and ring orbitals.

(2) The dimer formation, favored by the nitro group, induces a quenching in the vibrational modes that are responsible for the coupling of iron d and ring orbitals, interfering in the relaxation mechanism. This quenching does not exclude an antiferromagnetic coupling with both Fe(IV).

(3) The presence of the nitro group also favors route I (**A** → **B** → **C** → products). The absence of water in the system favors routes II and III, justifying the lack of radical signal in the EPR spectra, and a decrease in the yield of cyclohexanol.

It is clear to us that the detection and characterization of these very reactive intermediates is a valuable contribution to the understanding of the C–H activation in hydrocarbons important in biological and industrial processes.

Acknowledgements

This work was supported by CAPES, CNPq, FAPESP and FINEP. We thank Professors O. Baffa Filho and R. L. Zimmerman for helpful discussions.

References

1 J. T. Groves, R. C. Haushalter, M. Nakamura, T. E. Nemo and B. J. Evans, *J. Am. Chem. Soc., 103* (1981) 2884.

2 T. S. Calderwood, W. A. Lee and T. C. Bruice, *J. Am. Chem. Soc., 107* (1985) 8272.

3 J. E. Penner-Hahn, T. J. McMurry, M. Renner, L. Latos-Grazynsky, K. S. Eble, I. M. Davis, A. L. Balch, J. T. Groves, J. H. Dawson and K. O. Hodgson, *J. Biol. Chem., 258* (1983) 12761.
4 J. T. Groves and T. E. Nemo, *J. Am. Chem. Soc., 105* (1983) 6243.
5 D. L. Hickman, A. Nanthakumar and H. M. Goff, *J. Am. Chem. Soc., 110* (1988) 6384.
6 A. Gold, K. Jayaraj, P. Doppelt, R. Weiss, G. Chottard, E. Bill, X. Ding and A. X. Trautwein, *J. Am. Chem. Soc., 110* (1988) 5756.
7 J. T. Groves and Y. Watanabe, *J. Am. Chem. Soc., 110* (1988) 8443.
8 T. L. McDonald, L. T. Burka, S. T. Wright and F. P. Guengerich, *Biochem. Biophys. Res. Commun., 104* (1982) 620.
9 R. E. White and M. J. Coon, *Ann. Rev. Biochem., 49* (1980) 315.
10 J. H. Dawson and K. S. Eble, in A. G. Sykes (ed.), *Advances in Inorganic and Bioinorganic Mechanisms,* Vol. IV, Academic Press, New York, 1986, Ch. 1.
11 G. D. Nordblom, R. E. White and M. J. Coon, *Arch. Biochem. Biophys., 175* (1976) 524.
12 F. Lichtenberger, W. Nastainczyk and V. Ullrich, *Biochem. Biophys. Res. Commun., 70* (1976) 939.
13 P. R. Ortiz de Montellano, *Cytochrome P-450: Structure, Mechanism, and Biochemistry,* Plenum, New York, 1986.
14 F. P. Guengerich and T. L. MacDonald, *Acc. Chem. Res., 17* (1984) 9.
15 H. B. Dunford and J. S. Stillman, *Coord. Chem. Rev., 19* (1976) 187.
16 H. B. Dunford, *Adv. Inorg. Biochem., 4* (1982) 41.
17 M. D. Assis, *Ph.D. Dissertation,* University of São Paulo, Brazil, 1988.
18 J. P. Collman, J. I. Brauman, K. M. Doxsee, T. R. Halbert, E. Bunnenberg, R. E. Linder, G. N. LaMar, J. D. Gaudio, G. Lang and K. Spartalian, *J. Am. Chem. Soc., 102* (1980) 4182.
19 A. D. Adler, F. R. Longo, J. D. Finarelli, J. Goldmacher, J. Assour and L. Korsakoff, *J. Org. Chem., 32* (1967) 476.
20 A. D. Adler, F. R. Longo, F. Kampas and J. Kim, *J. Inorg. Nucl. Chem., 32* (1970) 2443.
21 J. G. Sharefkin and H. Saltzman, *Org. Synth., 43* (1963) 62.
22 G. M. Badger, R. A. Jones and R. L. Laslett, *Aust. J. Chem., 17* (1964) 1028.
23 E. B. Fleischer and T. S. Srivastava, *J. Am. Chem. Soc., 91* (1969) 2403.
24 R. J. Cheng, L. Latos-Grazynski and A. L. Balch, *Inorg. Chem., 21* (1982) 2412.
25 K. S. Murray, *Coord. Chem. Rev., 12* (1974) 1.
26 J. P. Mahy, P. Battioni, G. Bedi, D. Mansuy, J. Fischer, R. Weiss and I. Morgenstern-Badarau, *Inorg. Chem., 27* (1988) 353.
27 J. Fajer and M. S. Davis, in D. Dolphin (ed.), *The Porphyrins,* Vol. IV, Academic Press, New York, 1979, Ch. 4, p. 199.
28 P. Riesz, D. Berdahl and C. L. Christman, *Environ. Health Perspect., 64* (1985) 233.
29 T. D. Lash and D. Berry, *J. Chem. Educ., 62* (1985) 85.
30 C. E. Schulz, P. W. Devaney, H. Winkler, P. G. Debrunner, N. Doan, R. Chiang, R. Rutter and L. P. Hager, *FEBS Lett., 103* (1979) 102.
31 C. E. Schulz, R. Rutter, J. T. Sage, P. G. Debrunner and L. P. Hager, *Biochemistry, 23* (1984) 4743.
32 R. H. Felton, G. S. Owen, D. Dolphin, A. Forman, D. C. Borg and J. Fajer, *Ann. N.Y. Acad. Sci., 206* (1973) 504.
33 M. A. Phillippi and H. M. Goff, *J. Am. Chem. Soc., 104* (1982) 6026.
34 S. Hashimoto, Y. Tatsuno and T. Kitagawa, *J. Am. Chem. Soc., 109* (1987) 8096.
35 J. T. Groves and J. A. Gilbert, *Inorg. Chem., 25* (1986) 123.
36 W. F. Scholz, C. A. Reed, Y. J. Lee, W. R. Scheidt and G. Lang, *J. Am. Chem. Soc., 104* (1982) 6791.
37 G. Buisson, A. Deronzier, E. Duee, P. Gans, J. C. Marchon and J. R. Regnard, *J. Am. Chem. Soc., 104* (1982) 6793.
38 M. M. Williamson, C. M. Prosser-McCartha, S. Mukundan, Jr. and C. L. Hill, *Inorg. Chem., 27* (1988) 1061, and refs. therein.
39 D. Ostovic and T. C. Bruice, *J. Am. Chem. Soc., 111* (1989) 6511.
40 N. Sadasivan, H. I. Eberspaecher, W. H. Fuchsman and W. S. Caughey, *Biochemistry, 8* (1969) 534.
41 C. M. Dicken, P. N. Balasubramanian and T. C. Bruice, *Inorg. Chem., 27* (1988) 197.
42 H. C. Kelly and S. C. Yasui, *Inorg. Chem., 23* (1984) 3559.